

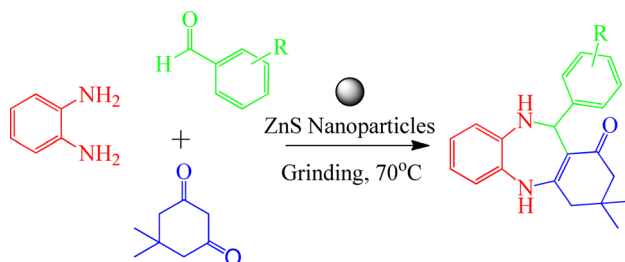
Facile three-component preparation of benzodiazepine derivatives catalyzed by zinc sulfide nanoparticles via grinding method

Hossein Naeimi¹ · Hossein Foroughi¹

Received: 15 April 2015 / Accepted: 28 August 2015
© Springer Science+Business Media Dordrecht 2015

Abstract In this research, ZnS nanoparticles were prepared and applied as heterogeneous reusable catalyst for synthesis of 1,5-benzodiazepines under grinding conditions at 70 °C. The multi-component reactions of aldehydes, dimedone and *o*-phenylenediamine were carried out under grinding conditions to obtain some 3,3-dimethyl-2,3,4,5,10,11-hexahydro-11-[aryl]-1H-dibenzo[*b,e*][1,4] diazepine-1-one derivatives. The present approach provides several advantages, including high yields, short reaction times, little catalyst loading and purification of compounds by crystallization method. The catalyst was characterized by using FT-IR, XRD, PL, EDX, SEM and TEM techniques.

Graphical Abstract



Electronic supplementary material The online version of this article (doi:10.1007/s11164-015-2254-4) contains supplementary material, which is available to authorized users.

✉ Hossein Naeimi
naeimi@kashanu.ac.ir

¹ Department of Organic Chemistry, Faculty of Chemistry, University of Kashan, Kashan 87317, Islamic Republic of Iran

Keywords 1,5-Benzodiazepines · ZnS nanoparticles · Dimedone · *o*-Phenylenediamine · Aromatic aldehyde · Grinding

Introduction

Multi-component reactions (MCRs) are those reactions whereby more than two reactants combine in a sequential manner to give highly selective products that retain a majority of atoms from the starting material [1–5]. MCRs are efficient, fast, environmentally friendly, practical and atom economic. They introduce an effective tool for providing different compounds with biological and pharmaceutical properties [6, 7], including heterocyclic compounds [8, 9]. Benzodiazepines are some of the applicable heterocyclic compounds that have gained extensive interest because of their wide usage in biological activities [10, 11]. Benzodiazepine compounds are extensively consumed psychoactive drugs worldwide due to their anxiolytic and anticonvulsant activity [12].

Some methods for the synthesis of 1,5-benzodiazepine derivatives have been reported in the literature via the condensation of one equivalent *o*-phenylenediamine with various aldehydes or ketones in the presence of a wide variety of catalysts, including SmI_2 in the presence of molecular sieves at room temperature [13], $\text{HBF}_4\text{-SiO}_2$ under solvent-free conditions [14], $\text{Yb}(\text{OTf})_3$ [15], SiO_2 [16], AcOH as catalyst under microwave irradiation [17], $\text{SiO}_2\text{-H}_2\text{SO}_4$ catalyst under grinding-microwave method [18], $\text{C}_6\text{F}_5\text{COOH}$ [19], $\text{Ga}(\text{OTf})_3$ in CH_3CN [20], amorphous mesoporous iron alumino phosphate (FeAIP-550) as catalyst under solvent-free condition [21], Fe_3O_4 nanoparticles [22], $\text{Hg}(\text{OTf})_2$ [23] and CF_3COOH in the presence of dehydroacetic acid (DHA) [24]. Furthermore, the synthesis of 4-substituted-1,5-benzodiazepine derivatives have been carried out by three-component condensation of *o*-phenylenediamine, dimedone and aldehydes by using AcOH in ethanol [25], acetic acid [26], oxalic acid in water [27], AcOH in water under microwave condition [28], acetic acid in toluene [29], H_2SO_4 [30], HCl [31] as Brønsted catalysts. Some of the other reported catalysts for this reaction are $\text{Er}(\text{OTf})_3$ in CH_3CN [32, 33] and AcOH in the presence of 2,2-dihydroxy-1-phenylethanone under microwave irradiation [34]. Also, the hetero-Cope

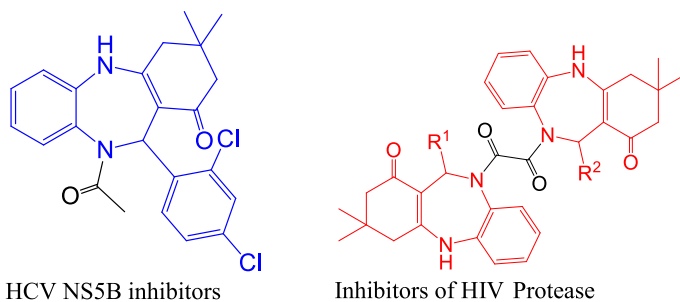


Fig. 1 Some examples of biologically 4-substituted-1,5-benzodiazepine derivatives

rearrangement protocol reported the synthesis of these compounds via condensation of 2-formyl benzoic acid with *o*-phenylenediamine and tetronic acid in water under microwave irradiation [28]. A unique gold (I)-catalyzed synthesis of 1,5-benzodiazepines directly from *o*-phenylenediamines and alkynes was achieved for the first time by Xu and co-workers [35], and was developed by Luo et al. [36]. Recently, the synthesis of benzodiazepines was reported by catalytic three-component coupling reaction of aromatic diamines, Meldrum's acid, and isocyanides [37]. In addition, acylchlorids were used for the synthesis of 4-substituted-1,5-benzodiazepine derivatives with medicinal properties [38–40] (Fig. 1).

In conjunction with ongoing to preparation of heterocyclic compounds, we report an efficient and novel method for the synthesis of 4-substituted-1,5-benzodiazepines via one-pot MCRs of *o*-phenylenediamine, dimedone and aldehyde derivatives. In this protocol, the aforesaid desired compounds were prepared in excellent yields and with short reaction times by using of ZnS NPs with specific surface to volume, crystalline size as a robust as well as effective and easily recoverable catalyst.

Experimental

Materials and techniques

All reagents were purchased from Merck, Aldrich, CDH and Fluka and were used without further purification. Fourier transform infrared (FT-IR) spectra were obtained as KBr pellets on a Perkin–Elmer 781 spectrophotometer. Ultraviolet (UV–Vis) spectra were obtained in CDCl_3 solvents on a Perkin–Elmer 550 S spectrophotometer. Nuclear magnetic resonance (^1H NMR and ^{13}C NMR) were recorded in DMSO and CDCl_3 solvents on a Bruker DRX-400 spectrometer with tetramethylsilane (TMS) as internal reference. The elemental analyses (C, H, N) were obtained from a Carlo ERBA Model EA 1108 analyzer. Electron Ionization Mass (EI-MASS) spectra were recorded on Agilent Technology (HP) 5973 instrument at an ionization potential of 70 eV. Nanostructures were characterized using a Holland Philips Xpert X-ray powder diffraction (XRD) diffractometer (CuK α , radiation, $k = 0.154056$ nm), at a scanning speed of $2^\circ/\text{min}$ from 10° to 100° (2θ). Electron Dispersive X-Ray (EDX) of nanoparticles was performed on a Zeiss Σ 1 GMA vp. Photoluminescence (PL) spectra were obtained on the Avantes Avaspec-2048 spectrophotometer. Scanning electron microscopy (SEM) of nanoparticles was performed on a KYKY EM-3200. Transmission electron microscopy (TEM) of nanoparticles was performed on a LEO AB-912. Melting points (MP) were obtained with a Thermo Scientific 9300. The purity determination of the substrates and reaction monitoring were accomplished by TLC on silica-gel polygram SILG/UV 254 plates (from Merck Company).

Preparation of ZnS NPs

In a typical procedure for synthesis of ZnS NPs, 1 mmol of $\text{Zn}(\text{OAc})_2 \cdot 2\text{H}_2\text{O}$ and 1 mmol of thioacetamide (TAA) were added into 20 ml ethylene glycol in a 50-ml

round-bottomed flask at room temperature. The solution was heated to 110 °C by microwave and the temperature was maintained for 5 min with stirring. After the solution was allowed to cool to room temperature naturally, the white crystalline ZnS nanoparticles were precipitated. The solid was separated, washed with absolute ethanol three times and dried at 60 °C for 3 h [41–45].

General procedure for synthesis of 4-substituted-1,5-benzodiazepines catalyzed by ZnS NPs

A mixture of *o*-phenylenediamine (1 mmol), dimedone (1 mmol) and selected aromatic aldehydes (1 mmol) in the presence of ZnS nanoparticles 10 mol% (0.01 g) was stirred in a mortar-pestle at 70 °C for appropriate times. During the procedure, the reaction was monitored by TLC (Thin Layer Chromatography). Upon completion, the reaction mixture was cooled to room temperature and the reaction mixture was dissolved in ethanol. The catalyst was insoluble in ethanol and easily centrifuged to separate. The solvent was evaporated and the obtained oil was crystallized from methanol and water (6:5) to afford the product. The residue was purified by recrystallization from ethanol. They were characterized by comparison of their physical and spectral data with those of authentic samples [30–40].

3,3-Dimethyl-2,3,4,5,10,11-hexahydro-11-[phenyl]-1H-dibenzo[b,e][1,4] diazepin-1-one (3a)

Pale green solid, yield: 84 %; m.p. = 246–248 °C; R_f = 0.125 (1:1 Ethylacetate/*n*-Hexane); UV–Vis: λ_{\max} = 360 nm; IR (KBr)/ ν (cm^{-1}): 3296, 3237, 3057, 2955, 1584, 1384, 1530, 1329, 1424, 1277; ^1H NMR (DMSO + CDCl_3 , 400 MHz)/ δ (ppm): 1.03 (s, 3H, CH_3 –), 1.08 (s, 3H, CH_3 –), 2.11 (A.B q, 2H, J = 16.0 Hz, CH_2), 2.56 (s, 2H, $-\text{CH}_2-\text{C}=\text{O}$), 5.71 (s, 1H, N–H), 6.08 (s, 1H, C–H), 6.47–6.57 (m, 3H, Ar–), 6.89 (d, 1H, J = 8.0 Hz, Ar–), 6.95 (t, 1H, J = 8.0 Hz Ar–), 7.0–7.1 (m, 3H, Ar–), 8.15 (d, 1H, J = 4.0 Hz, Ar–), 8.69 (s, 1H, N–H); ^{13}C NMR (DMSO + CDCl_3 , 100 MHz)/ δ (ppm): 27.95, 29.06, 32.21, 44.74, 50.05, 56.49, 110.68, 119.87, 120.44, 121.01, 122.98, 126.11, 127.7, 127.98, 131.49, 138.84, 145.1, 155.12, 192.52; EI-MASS (m/z , %): 318 (M^+ , 26), 241 (100), 149 (52), 83 (45), 77 (34), 57 (85), 55 (62); Anal. Calcd. For $\text{C}_{21}\text{H}_{22}\text{N}_2\text{O}$: C 79.21, H 6.96, N 8.80, Found C 79.24, H 6.98, N 8.84.

3,3-Dimethyl-2,3,4,5,10,11-hexahydro-11-[(4-nitro)phenyl]-1H-dibenzo[b,e][1,4] diazepin-1-one (3b)

Yellow solid, yield: 89 %; m.p. = 280–281 °C (decomp); R_f = 0.125 (1:1 Ethylacetate/*n*-Hexane); UV–Vis: λ_{\max} = 348 nm; IR (KBr)/ ν (cm^{-1}): 3355, 3279, 3181, 2955, 1591, 1381, 1511, 1339, 1425, 1275; ^1H NMR (DMSO + CDCl_3 , 400 MHz)/ δ (ppm): 0.99 (s, 3H, CH_3 –), 1.06 (s, 3H, CH_3 –), 2.14 (A.B q, 2H, J = 16.0 Hz, CH_2 –), 2.53 (s, 2H, $-\text{CH}_2-\text{C}=\text{O}$), 5.64 (s, 1H, N–H), 5.87 (s, 1H, C–H), 6.43 (d, 1H, J = 6.4 Hz, Ar–), 6.55–6.61 (m, 2H, Ar–), 6.9 (d, 1H, J = 6.4 Hz, Ar–), 7.21 (d, 2H, J = 8.8 Hz, Ar–), 7.84 (d, 2H, J = 8.8 Hz, Ar–),

8.58 (s, 1H, N-H); ^{13}C NMR (DMSO + CDCl_3 , 100 MHz)/ δ (ppm): 28.09, 28.80, 32.20, 44.82, 49.93, 56.63, 109.44, 120.52, 120.75, 121.09, 123.08, 123.43, 128.57, 131.39, 138.03, 146.05, 153.05, 155.05, 192.85; EI-MASS (m/z , %): 397 (M^+ , 29), 241 (100), 149 (66), 83 (51), 77 (32), 57 (39), 55 (47); Anal. Calcd. For $\text{C}_{21}\text{H}_{21}\text{N}_3\text{O}_3$: C 69.41, H 5.82, N 11.56, Found C 69.45, H 5.85, N 11.59.

3,3-Dimethyl-2,3,4,5,10,11-hexahydro-11-[(2-nitro)phenyl]-1H-dibenzo[b,e][1,4]diazepin-1-one (3c)

Orange solid, yield: 88 %; m.p. = 230–232 °C (decomp); R_f = 0.281 (1:1 Ethylacetate/*n*-Hexane); UV-Vis: λ_{max} = 346 nm; IR (KBr)/ ν (cm^{-1}): 3378, 3303, 3069, 2957, 1591, 1381, 1528, 1332, 1473, 1279; ^1H NMR (DMSO + CDCl_3 , 400 MHz)/ δ (ppm): 0.95 (s, 3H, CH_3 -), 1.05 (s, 3H, CH_3 -), 2.01 (A.Bq, 2H, J = 16.0 Hz, CH_2 -), 2.58 (s, 2H, $-\text{CH}_2-\text{C}=\text{O}$), 5.04 (s, 1H, N-H), 6.01 (s, 1H, C-H), 6.32 (d, 1H, J = 8.0 Hz, Ar-), 6.58 (t, 1H, J = 8.0 Hz, Ar-), 6.67 (t, 1H, J = 8.0 Hz, Ar-), 6.79 (d, 1H, J = 8.0 Hz, Ar-), 7.04 (d, 1H, J = 8.0 Hz, Ar-), 7.14–7.2 (m, 2H, Ar-), 7.74 (d, 1H, J = 8.0 Hz, Ar-), 8.91 (s, 1H, N-H); ^{13}C NMR (DMSO + CDCl_3 , 100 MHz)/ δ (ppm): 28.11, 28.82, 32.22, 44.87, 49.91, 56.62, 109.46, 120.53, 120.78, 121.07, 123.1, 123.46, 126.14, 128.56, 128.59, 131.38, 138.06, 146.03, 153.08, 155.08, 192.89; EI-MASS (m/z , %): 363 (M^+ , 26), 241 (100), 149 (55), 83 (36), 77 (42), 57 (49), 55 (62); Anal. Calcd. For $\text{C}_{21}\text{H}_{21}\text{N}_3\text{O}_3$: C 69.41, H 5.82, N 11.56, Found C 69.46, H 5.85, N 11.60.

3,3-Dimethyl-2,3,4,5,10,11-hexahydro-11-[(3-nitro)phenyl]-1H-dibenzo[b,e][1,4]diazepin-1-one (3d)

Pale yellow solid, yield: 88 %; m.p. = 195–197 °C; R_f = 0.125 (1:1 Ethylacetate/*n*-Hexane); UV-Vis: λ_{max} = 348 nm; IR (KBr)/ ν (cm^{-1}): 3375, 3328, 3049, 2959, 1589, 1383, 1529, 1345, 1431, 1277; ^1H NMR (DMSO + CDCl_3 , 400 MHz)/ δ (ppm): 1.05 (s, 3H, CH_3 -), 1.09 (s, 3H, CH_3 -), 2.14 (A.Bq, 2H, J = 16.0 Hz, CH_2 -), 2.58 (s, 2H, $-\text{CH}_2-\text{C}=\text{O}$), 5.81 (s, 1H, N-H), 6.20 (s, 1H, C-H), 6.50 (d, 1H, J = 5.2 Hz, Ar-), 6.51–6.6 (m, 2H, Ar-), 6.9 (d, 1H, J = 7.2 Hz, Ar-), 7.29 (t, 1H, J = 8.0 Hz, Ar-), 7.45 (d, 1H, J = 8.0 Hz, Ar-), 7.81 (d, 1H, J = 9.2 Hz, Ar-), 7.98 (s, 1H, Ar-), 8.79 (s, 1H, N-H); ^{13}C NMR (DMSO + CDCl_3 , 100 MHz)/ δ (ppm): 28.1, 28.81, 32.24, 44.86, 49.93, 56.64, 109.47, 120.56, 120.76, 121.06, 123.11, 123.47, 126.16, 128.49, 128.56, 131.39, 138.09, 146.05, 153.1, 155.09, 192.86; EI-MASS (m/z , %): 363 (M^+ , 30), 241 (100), 149 (38), 83 (40), 77 (41), 57 (39), 55 (58); Anal. Calcd. For $\text{C}_{21}\text{H}_{21}\text{N}_3\text{O}_3$: C 69.41, H 5.82, N 11.56, Found C 69.45, H 5.86, N 11.57.

3,3-Dimethyl-2,3,4,5,10,11-hexahydro-11-[(4-chloro)phenyl]-1H-dibenzo[b,e][1,4]diazepin-1-one (3e)

Pale green solid, yield: 85 %; m.p. = 235–237 °C; R_f = 0.125 (1:1 Ethylacetate/*n*-Hexane); UV-Vis: λ_{max} = 344 nm; IR (KBr)/ ν (cm^{-1}): 3301, 3238, 3054, 2956, 1587, 1381, 1532, 1329, 1426, 1278; ^1H NMR (DMSO + CDCl_3 , 400 MHz)/ δ

(ppm): 1.0 (s, 3H, CH₃-), 1.06 (s, 3H, CH₃-), 2.11 (A.Bq, 2H, $J = 16.0$ Hz, CH₂-), 2.52 (s, 2H, -CH₂-C=O), 5.73 (s, 1H, N-H), 5.78 (s, 1H, C-H), 6.45 (d, 1H, $J = 8.2$ Hz, Ar-), 6.55 (m, 2H, Ar-), 6.88 (d, 1H, $J = 8.2$ Hz, Ar-), 6.98 (d, 2H, $J = 8.4$ Hz, Ar-), 7.01 (d, 1H, $J = 8.4$ Hz, Ar-), 8.61 (s, 1H, N-H); ¹³C NMR (DMSO + CDCl₃, 100 MHz)/ δ (ppm): 28.17, 28.69, 32.24, 44.84, 49.90, 56.43, 109.38, 120.62, 120.72, 121.05, 123.11, 123.28, 128.36, 131.45, 138.06, 146.08, 150.02, 152.06, 192.81; EI-MASS (m/z , %): 362 (M⁺, 33), 354 (M+2⁺, 11), 241 (100), 149 (57), 83 (35), 77 (28), 57 (68), 55 (53); Anal. Calcd. For C₂₁H₂₁ClN₂O: C 71.48, H 6.0, N 7.94, Found C 71.53, H 6.5, N 7.98.

3,3-Dimethyl-2,3,4,5,10,11-hexahydro-11-[(2-chloro)phenyl]-1H-dibenzo[b,e][1,4]diazepin-1-one (3f)

White solid, yield: 86 %; m.p. = 239–240 °C (decomp); $R_f = 0.281$ (1:1 Ethylacetate/*n*-Hexane); UV-Vis: $\lambda_{\max} = 348$ nm; IR (KBr)/ ν (cm⁻¹): 3292, 3235, 3062, 2959, 1589, 1382, 1515, 1314, 1422, 1278; ¹H NMR (DMSO + CDCl₃, 400 MHz)/ δ (ppm): 1.02 (s, 3H, CH₃-), 1.07 (s, 3H, CH₃-), 2.09 (A.Bq, 2H, $J = 16.0$ Hz, CH₂-), 2.57 (s, 2H, -CH₂-C=O), 5.07 (s, 1H, N-H), 6.01 (s, 1H, C-H), 6.33 (d, 1H, $J = 7.2$ Hz, Ar-), 6.44–6.62 (m, 2H, Ar-), 6.7 (d, 1H, $J = 7.6$ Hz, Ar-), 6.82 (d, 1H, $J = 7.6$ Hz, Ar-), 6.85–7.0 (m, 2H, Ar-), 7.20 (d, $J = 7.6$ Hz, 1H, Ar-), 8.77 (s, 1H, N-H); ¹³C NMR (DMSO + CDCl₃, 100 MHz)/ δ (ppm): 28.17, 28.72, 32.26, 44.84, 49.88, 56.42, 109.32, 120.61, 120.66, 121.12, 123.13, 123.42, 126.11, 128.53, 128.62, 131.42, 138.04, 146.06, 149.55, 151.06, 192.82; EI-MASS (m/z , %): 352 (M⁺, 36), 354 (M+2⁺, 12), 241 (100), 149 (52), 83 (49), 77 (33), 57 (42), 55 (51); Anal. Calcd. For C₂₁H₂₁ClN₂O: C 71.48, H 6.0, N 7.94, Found C 71.54, H 6.6, N 7.99.

3,3-Dimethyl-2,3,4,5,10,11-hexahydro-11-[(2,3-dichloro)phenyl]-1H-dibenzo[b,e][1,4]diazepin-1-one (3g)

Pale green solid, yield: 89 %; m.p. = 256–358 °C (decomp); $R_f = 0.281$ (1:1 Ethylacetate/*n*-Hexane); UV-Vis: $\lambda_{\max} = 348$ nm; IR (KBr)/ ν (cm⁻¹): 3379, 3301, 3060, 2958, 1589, 1380, 1532, 1332, 1423, 1289; ¹H NMR (DMSO + CDCl₃, 400 MHz)/ δ (ppm): 1.01 (s, 3H, CH₃-), 1.07 (s, 3H, CH₃-), 2.12 (A.Bq, 2H, $J = 16.0$ Hz, CH₂-), 2.56 (s, 2H, -CH₂-C=O), 4.96 (s, 1H, N-H), 6.07 (s, 1H, C-H), 6.30 (d, 1H, $J = 7.6$ Hz, Ar-), 6.53–6.60 (m, 2H, Ar-), 6.62 (d, 1H, $J = 7.2$ Hz, Ar-), 6.75 (t, 1H, $J = 8.0$ Hz, Ar-), 6.91 (d, 1H, $J = 7.6$ Hz, Ar-), 7.08 (d, 1H, $J = 7.6$ Hz, Ar-), 8.64 (s, 1H, N-H); ¹³C NMR (DMSO + CDCl₃, 100 MHz)/ δ (ppm): 28.14, 28.67, 32.23, 44.81, 49.92, 56.29, 109.10, 120.68, 121.08, 121.35, 123.65, 126.13, 126.84, 128.83, 131.71, 132.05, 132.57, 137.33, 143.52, 156.12, 192.90; EI-MASS (m/z , %): 386 (M⁺, 24), 388 (M+2⁺, 14), 390 (M+4⁺, 4), 351 (52), 241 (100), 149 (25), 83 (34), 77 (24), 69 (52), 57 (43), 55 (54); Anal. Calcd. For C₂₁H₂₀Cl₂N₂O: C 65.12, H 5.20, N 7.23 Found C 65.15, H 5.24, N 7.26.

3,3-Dimethyl-2,3,4,5,10,11-hexahydro-11-[(2,4-dichloro)phenyl]-1H-dibenzo[b,e][1,4] diazepin-1-one (3h)

Pale green solid, yield: 90 %; m.p. = 230–232 °C (decomp); R_f = 0.281 (1:1 Ethylacetate/*n*-Hexane); UV–Vis: λ_{\max} = 347 nm; IR (KBr)/ ν (cm^{-1}): 3303, 3241, 3055, 2957, 1590, 1382, 1533, 1330, 1468, 1278; ^1H NMR (DMSO + CDCl_3 , 400 MHz)/ δ (ppm): 1.02 (s, 3H, CH_3 –), 1.07 (s, 3H, CH_3 –), 2.11 (A.Bq, 2H, J = 16.0 Hz, CH_2 –), 2.57 (s, 2H, $-\text{CH}_2-\text{C}=\text{O}$), 4.99 (s, 1H, N–H), 5.99 (s, 1H, C–H), 6.34 (d, 1H, J = 7.6 Hz, Ar–), 6.56–6.63 (m, 2H, Ar–), 6.65 (d, 1H, J = 8.4 Hz, Ar–), 6.79 (d, 1H, J = 8.0 Hz, Ar–), 6.92 (d, 1H, J = 7.2 Hz, Ar–), 7.22 (s, 1H, Ar–), 8.74 (s, 1H, N–H); ^{13}C NMR (DMSO + CDCl_3 , 100 MHz)/ δ (ppm): 28.16, 28.69, 32.26, 44.78, 49.93, 56.31, 109.12, 120.72, 121.06, 121.37, 123.68, 126.15, 126.88, 128.87, 131.68, 132.04, 132.59, 137.38, 149.57, 156.18, 192.92; EI-MASS (m/z , %): 386 (M^+ , 26), 388 ($\text{M}+2^+$, 16), 390 ($\text{M}+4^+$, 6), 241 (100), 149 (66), 83 (57), 77 (30), 57 (65), 55 (45); Anal. Calcd. For $\text{C}_{21}\text{H}_{20}\text{Cl}_2\text{N}_2\text{O}$: C 65.12, H 5.20, N 7.23, Found C 65.16, H 5.25, N 7.28.

3,3-Dimethyl-2,3,4,5,10,11-hexahydro-11-[(4-chloro-3-nitro)phenyl]-1H-dibenzo[b,e][1,4] diazepin-1-one (3i)

Pale yellow solid, yield: 87 %; m.p. = 196–197 °C; R_f = 0.125 (1:1 Ethylacetate/*n*-Hexane); UV–Vis: λ_{\max} = 348 nm; IR (KBr)/ ν (cm^{-1}): 3305, 3240, 3039, 2958, 1600, 1381, 1532, 1339, 1426, 1276; ^1H NMR (DMSO + CDCl_3 , 400 MHz)/ δ (ppm): 1.02 (s, 3H, CH_3 –), 1.07 (s, 3H, CH_3 –), 2.13 (A.Bq, 2H, J = 16.0 Hz, CH_2 –), 2.54 (s, 2H, $-\text{CH}_2-\text{C}=\text{O}$), 5.77 (s, 1H, N–H), 6.08 (s, 1H, C–H), 6.50 (d, 1H, J = 8.0 Hz, Ar–), 6.59 (m, 2H, Ar–), 6.91 (d, 1H, J = 8.0 Hz, Ar–), 7.24–7.29 (m, 2H, Ar–), 7.68 (s, 1H, Ar–), 8.74 (s, 1H, N–H); ^{13}C NMR (DMSO + CDCl_3 , 100 MHz)/ δ (ppm): 28.04, 28.75, 32.19, 44.69, 49.84, 56.02, 109.07, 120.75, 120.85, 121.18, 123.36, 123.63, 124.85, 131.21, 131.44, 132.66, 138.04, 146.18, 147.33, 155.94, 192.9; EI-MASS (m/z , %): 397 (M^+ , 21), 399 ($\text{M}+2^+$, 4), 241 (100), 149 (47), 83 (47), 77 (27), 69 (81), 57 (91), 55 (67); Anal. Calcd. For $\text{C}_{21}\text{H}_{20}\text{ClN}_3\text{O}_3$: C 63.40, H 5.07, N 10.56, Found C 63.46, H 5.13, N 10.64.

3,3-Dimethyl-2,3,4,5,10,11-hexahydro-11-[(4-methyl)phenyl]-1H-dibenzo[b,e][1,4] diazepin-1-one (3j)

Pale green solid, yield: 85 %; m.p. = 224–226 °C; R_f = 0.125 (1:1 Ethylacetate/*n*-Hexane); UV–Vis: λ_{\max} = 361 nm; IR (KBr)/ ν (cm^{-1}): 3307, 3245, 3050, 2959, 1595, 1380, 1538, 1327, 1471, 1276; ^1H NMR (DMSO + CDCl_3 , 400 MHz)/ δ (ppm): 1.01 (s, 3H, CH_3 –), 1.07 (s, 3H, CH_3 –), 2.01 (A.Bq, 2H, J = 16.0 Hz, CH_2 –), 2.01 (s, 3H, Me–), 2.52 (s, 2H, $-\text{CH}_2-\text{C}=\text{O}$), 5.69 (s, 1H, N–H), 5.69 (s, 1H, C–H), 6.45 (d, 1H, J = 7.6 Hz, Ar–), 6.5–6.6 (m, 2H, Ar–), 6.81 (d, 2H, J = 7.6 Hz, Ar–), 6.86 (d, 1H, J = 8.0 Hz, Ar–), 6.92 (d, J = 7.6 Hz, 2H, Ar–), 8.53 (s, 1H, N–H); ^{13}C NMR (DMSO + CDCl_3 , 100 MHz)/ δ (ppm): 27.85, 29.16, 32.23, 44.71, 50.09, 55.07, 56.51, 110.69, 119.86, 120.47, 121.07, 122.96, 126.35, 127.58, 127.94, 131.53, 138.87, 145.11, 155.14, 192.56; EI-MASS (m/z , %): 332

(M^+ , 43), 241 (100), 149 (55), 83 (39), 77 (41), 57 (77), 55 (46); Anal. Calcd. For $C_{22}H_{24}N_2O$: C 79.48, H 7.28, N 8.43, Found C 79.53, H 7.35, N 8.49.

3,3-Dimethyl-2,3,4,5,10,11-hexahydro-11-[(4-methoxy)phenyl]-1H-dibenzo[b,e][1,4]diazepin-1-one (3k)

Pale cream solid, yield: 82 %; m.p. = 229–231 °C; R_f = 0.125 (1:1 Ethylacetate/*n*-Hexane); UV–Vis: λ_{max} = 364 nm; IR (KBr)/ ν (cm^{-1}): 3301, 3238, 3015, 2956, 1587, 1382, 1535, 1327, 1426, 1279; 1H NMR (DMSO + $CDCl_3$, 400 MHz)/ δ (ppm): 1.01 (s, 3H, CH_3-), 1.06 (s, 3H, CH_3-), 2.10 (s, 3H, Me-), 2.10 (s, 1H, C–H), 2.11 (A.Bq, 2H, J = 16.0 Hz, CH_2-), 2.52 (s, 2H, $-CH_2-C=O$), 5.7 (s, 1H, N–H), 6.45 (d, 1H, J = 7.6 Hz, Ar-), 6.5–6.58 (m, 2H, Ar-), 6.81 (d, 2H, J = 8.0 Hz, Ar-), 6.87 (d, 1H, J = 8.4 Hz, Ar-), 6.91 (d, J = 8.0 Hz, 2H, Ar-), 8.55 (s, 1H, N–H); ^{13}C NMR (DMSO + $CDCl_3$, 100 MHz)/ δ (ppm): 27.82, 29.19, 32.23, 44.75, 50.04, 54.11, 56.42, 110.67, 111.46, 113.56, 119.93, 120.41, 121.05, 123.06, 128.89, 131.46, 138.89, 146.66, 155.21, 192.08; EI-MASS (m/z , %): 348 (M^+ , 67), 241 (100), 149 (36), 83 (35), 77 (42), 57 (43), 55 (52); Anal. Calcd. For $C_{22}H_{24}N_2O_2$: C 75.83, H 6.94, N 8.04, Found C 75.86, H 6.97, N 8.07.

3,3-Dimethyl-2,3,4,5,10,11-hexahydro-11-[(2-methoxy)phenyl]-1H-dibenzo[b,e][1,4]diazepin-1-one (3l)

Pale cream solid, yield: 83 %; m.p. = 217–218 °C (decomp); R_f = 0.125 (1:1 Ethylacetate/*n*-Hexane); UV–Vis: λ_{max} = 361 nm; IR (KBr)/ ν (cm^{-1}): 3369, 3306, 3063, 2955, 1599, 1384, 1534, 1327, 1425, 1236; 1H NMR (DMSO + $CDCl_3$, 400 MHz)/ δ (ppm): 1.07 (s, 3H, CH_3-), 1.08 (s, 3H, CH_3-), 2.12 (A.Bq, 2H, J = 16.0 Hz, CH_2-), 2.57 (s, 2H, $-CH_2-C=O$), 3.89 (s, 3H, Me-), 5.0 (s, 1H, N–H), 5.95 (s, 1H, C–H), 6.28 (d, 1H, J = 7.6 Hz, Ar-), 6.45–6.55 (m, 3H, Ar-), 6.58 (d, 1H, J = 7.6 Hz, Ar-), 6.75 (d, 1H, J = 8.4 Hz, Ar-), 6.86 (d, J = 7.6 Hz, 1H, Ar-), 6.94 (t, 1H, J = 8.0 Hz, Ar-), 8.59 (s, 1H, N–H); ^{13}C NMR (DMSO + $CDCl_3$, 100 MHz)/ δ (ppm): 27.95, 29.08, 32.32, 44.77, 50.05, 54.79, 56.43, 110.75, 111.47, 113.56, 119.89, 120.06, 120.40, 121.05, 123.06, 128.85, 131.47, 138.86, 146.65, 155.26, 159.24, 192.65; EI-MASS (m/z , %): 348 (M^+ , 42), 241 (100), 149 (52), 83 (61), 77 (27), 57 (85), 55 (72); Anal. Calcd. For $C_{22}H_{24}N_2O_2$: C 75.83, H 6.94, N 8.04, Found C 75.9, H 6.98, N 8.10.

3,3-Dimethyl-2,3,4,5,10,11-hexahydro-11-[(3-methoxy)phenyl]-1H-dibenzo[b,e][1,4]diazepin-1-one (3m)

Pale green solid, yield: 84 %; m.p. = 225–227 °C; R_f = 0.125 (1:1 Ethylacetate/*n*-Hexane); UV–Vis: λ_{max} = 364 nm; IR (KBr)/ ν (cm^{-1}): 3326, 3278, 3050, 2954, 1586, 1382, 1538, 1332, 1497, 1274; 1H NMR (DMSO + $CDCl_3$, 400 MHz)/ δ (ppm): 1.01 (s, 3H, CH_3-), 1.06 (s, 3H, CH_3-), 2.12 (A.Bq, 2H, J = 16.0 Hz, CH_2-), 2.52 (s, 2H, $-CH_2-C=O$), 3.55 (s, 3H, Me-), 5.64 (s, 1H, N–H), 5.72 (s, 1H, C–H), 6.44–6.48 (m, 2H, Ar-), 6.53–6.57 (m, 2H, Ar-), 6.60 (s, 1H, Ar-), 6.62 (d, 1H, J = 8.0 Hz, Ar-), 6.86 (d, 1H, J = 7.6 Hz, Ar-), 6.91 (t, 1H, J = 8.0 Hz, Ar-),

8.53 (s, 1H, N-H); ^{13}C NMR (DMSO + CDCl_3 , 100 MHz)/ δ (ppm): 27.81, 29.18, 32.21, 44.72, 50.02, 54.99, 56.41, 110.64, 111.44, 113.54, 119.91, 120.08, 120.43, 121.03, 123.03, 128.87, 131.44, 138.87, 146.63, 155.24, 159.25, 192.60; EI-MASS (m/z , %): 348 (M^+ , 72), 241 (100), 149 (45), 83 (31), 77 (37), 69 (34), 57 (35), 55 (42); Anal. Calcd. For $\text{C}_{22}\text{H}_{24}\text{N}_2\text{O}_2$: C 75.83, H 6.94, N 8.04, Found C 75.86, H 6.97, N 8.07.

3,3-Dimethyl-2,3,4,5,10,11-hexahydro-11-[(2-hydroxy)phenyl]-1H-dibenzo[b,e][1,4]diazepin-1-one (3n)

Pale cream solid, yield: 84 %; m.p. = 201–202 °C; R_f = 0.125 (1:1 Ethylacetate/*n*-Hexane); UV-Vis: λ_{max} = 360 nm; IR (KBr)/ ν (cm^{-1}): 3622, 3302, 3238, 3100, 2957, 1599, 1384, 1528, 1328, 1424, 1276; ^1H NMR (DMSO + CDCl_3 , 400 MHz)/ δ (ppm): 1.06 (s, 3H, CH_3 -), 1.08 (s, 3H, CH_3 -), 2.13 (A.Bq, 2H, J = 16.0 Hz, CH_2 -), 2.56 (s, 2H, $-\text{CH}_2-\text{C}=\text{O}$), 5.18 (s, 1H, N-H), 5.93 (s, 1H, C-H), 6.35 (t, 2H, J = 7.2 Hz, Ar), 6.38 (d, 1H, J = 6.8 Hz, Ar-), 6.50–6.55 (m, 3H, Ar-), 6.66 (d, 1H, J = 8.0 Hz, Ar-), 6.76 (t, 1H, J = 7.2 Hz, Ar-), 6.86 (d, J = 7.2 Hz, 1H, Ar-), 8.53 (s, 1H, N-H), 9.35 (s, 1H, O-H); ^{13}C NMR (DMSO + CDCl_3 , 100 MHz)/ δ (ppm): 28.04, 29.05, 32.22, 44.71, 50.11, 56.39, 110.89, 113.22, 115.08, 118.65, 119.77, 120.43, 120.96, 122.97, 128.71, 131.47, 138.95, 146.62, 155.07, 157.26, 192.55; EI-MASS (m/z , %): 348 (M^+ , 23), 241 (100), 149 (47), 83 (35), 77 (46), 57 (40), 55 (48); Anal. Calcd. For $\text{C}_{21}\text{H}_{22}\text{N}_2\text{O}_2$: C 75.42, H 6.63, N 8.38, Found C 75.47, H 6.68, N 8.43.

3,3-Dimethyl-2,3,4,5,10,11-hexahydro-11-[(3-hydroxy)phenyl]-1H-dibenzo[b,e][1,4]diazepin-1-one (3o)

Pale green solid, yield: 81 %; m.p. = 287–289 °C (decomp); R_f = 0.125 (1:1 Ethylacetate/*n*-Hexane); UV-Vis: λ_{max} = 348 nm; IR (KBr)/ ν (cm^{-1}): 3447, 3307, 3048, 2927, 1585, 1386, 1519, 1332, 1425, 1275; ^1H NMR (DMSO + CDCl_3 , 400 MHz)/ δ (ppm): 1.03 (s, 3H, CH_3 -), 1.08 (s, 3H, CH_3 -), 2.11 (A.Bq, 2H, J = 16.0 Hz, CH_2 -), 2.54 (s, 2H, $-\text{CH}_2-\text{C}=\text{O}$), 5.60 (s, 1H, N-H), 5.94 (s, 1H, C-H), 6.37 (d, 1H, J = 7.6 Hz, Ar-), 6.48–6.57 (m, 5H, Ar-), 6.82 (t, 1H, J = 7.6 Hz, Ar-), 6.89 (d, 1H, J = 7.6 Hz, Ar-), 8.64 (s, 1H, N-H), 8.90 (s, 1H, O-H); ^{13}C NMR (DMSO + CDCl_3 , 100 MHz)/ δ (ppm): 28.02, 29.09, 32.20, 44.74, 50.07, 56.36, 110.86, 113.19, 115.05, 118.60, 119.75, 120.39, 120.98, 122.94, 128.74, 131.43, 138.93, 146.59, 155.04, 157.21, 192.50; EI-MASS (m/z , %): 334 (M^+ , 34), 241 (100), 149 (61), 83 (57), 77 (25), 69 (84), 57 (90), 55 (72); Anal. Calcd. For $\text{C}_{21}\text{H}_{22}\text{N}_2\text{O}_2$: C 75.42, H 6.63, N 8.38, Found C 75.46, H 6.66, N 8.42.

11-(4-Chlorophenyl)-3,3,9-trimethyl-2,3,4,5,10,11-hexahydro-1H-dibenzo[b,e][1,4]diazepin-1-one

Yellowish solid, yield: 80 %; m.p. = 230–234 °C; R_f = 0.105 (1:1 Ethylacetate/*n*-Hexane); UV-Vis: λ_{max} = 332 nm; IR (KBr)/ ν (cm^{-1}): 3507, 3108, 3084, 2895, 1562, 1542, 1521, 1362, 1408, 1265; ^1H NMR (DMSO + CDCl_3 , 400 MHz)/ δ

(ppm): 1.11 (s, 3H, CH₃-), 1.20 (s, 3H, CH₃-), 2.07 (m, 2H, CH₂-), 2.24 (s, 3H, CH₃-Ar), 2.63 (s, 2H, -CH₂-C=O), 5.81 (s, 1H, C-H), 6.62 (d, 1H, *J* = 7.7 Hz, Ar-), 6.79 (s, 1H, Ar-), 6.95 (d, 1H, *J* = 7.7 Hz, Ar-), 7.06 (d, 2H, *J* = 8.1 Hz, Ar-), 7.24 (d, 1H, *J* = 8.1 Hz, Ar-), 8.62 (br, 2H, N-H); ¹³C NMR (DMSO + CDCl₃, 100 MHz)/δ (ppm): 20.15, 26.15, 26.19, 34.19, 45.01, 50.35, 55.08, 110.01, 121.35, 122.04, 122.38, 124.20, 124.87, 129.45, 132.81, 133.74, 147.25, 152.67, 153.42, 195.47; Anal. Calcd. For C₂₂H₂₃ClN₂O: C 72.02, H 6.32, Cl 9.66, N 7.64, Found C 71.84, H 6.01, N 7.40.

Results and discussion

ZnS nanoparticles were prepared according to the procedure of previously reported works [41–44, 46] from the reaction of Zn(OAc)₂·2H₂O and thioacetamide (TAA) with ethylene glycol under microwave irradiation and were used as heterogeneous catalyst in the organic reaction (Scheme 1).

Catalyst characterization

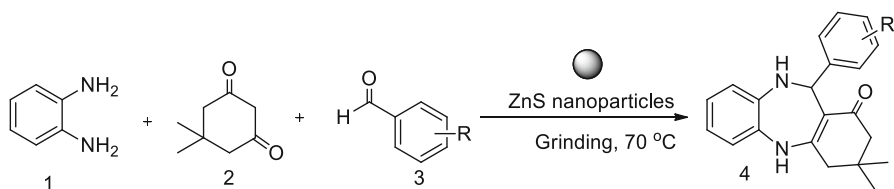
FT-IR studies

The FT-IR spectra (Fig. 2) of ZnS NPs samples showed very low absorption bands at 478, 1050 and 1415 cm⁻¹, which were assigned to the fundamental stretching and bending vibrations of related to Zn–S bond. A broad intense absorption between 3000 and 3700 cm⁻¹ is observed due to O–H vibration of water molecules, as characterized by its bending vibration at 1627 cm⁻¹ [41–44, 46].

PL studies

Photo-luminescent (PL) spectrum is an important tool to evaluate the defects and optical properties of ZnS NPs as a photonic material [45]. Furthermore, photoluminescence spectrum is sensitive to synthetic conditions, size, and shape of NPs.

Figure 3 shows the PL spectra of ZnS NPs recorded with an absorbance wavelength of 300 nm at room temperature. Broadening of the absorption peak could be attributed to both size distribution and increase in the surface states, owing to the increase in surface to volume ratio for ZnS NPs. Also, the results of PL



Scheme 1 Synthesis of 4-substituted-1,5-benzodiazepine under grinding conditions

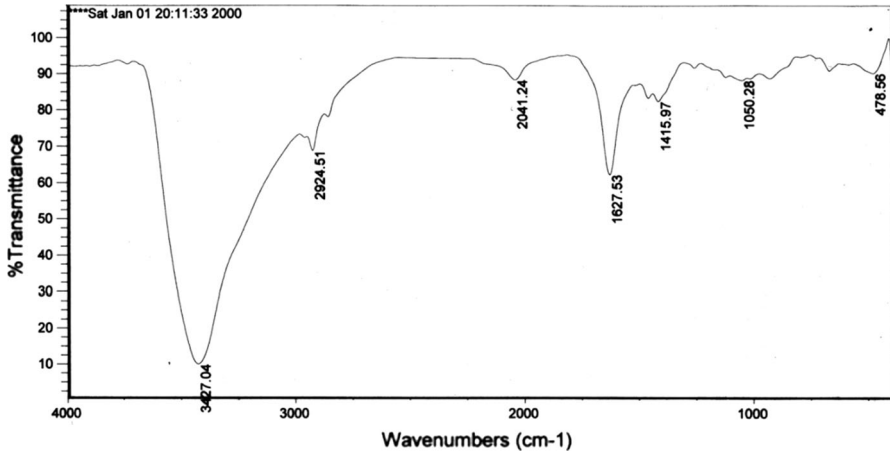


Fig. 2 The IR spectrum of ZnS NPs catalyst

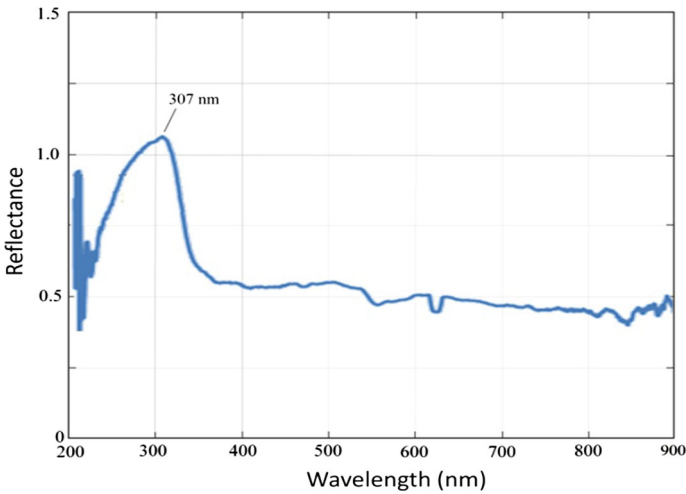


Fig. 3 The PL spectrum of ZnS NPs catalyst

spectra are consistent with those of XRD, which indicate particles with better crystalline and apposite size.

Powder X-ray diffraction technique (XRD)

The X-ray diffraction patterns of ZnS nanoparticles are shown in Fig. 4. The position and relative intensities of all peaks confirm well with the standard XRD pattern of ZnS nanoparticles, indicating retention of the crystalline cubic spinel structure during of NPs. The average NPs core diameter was calculated to be 6 nm

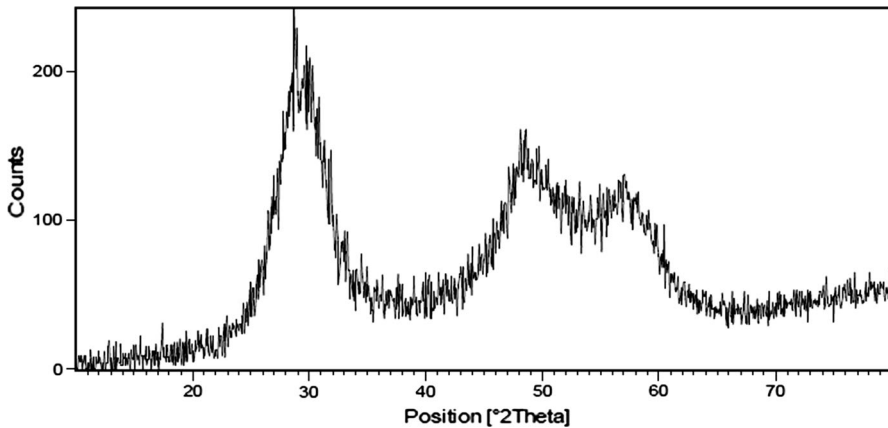


Fig. 4 The XRD patterns of ZnS NPs catalyst

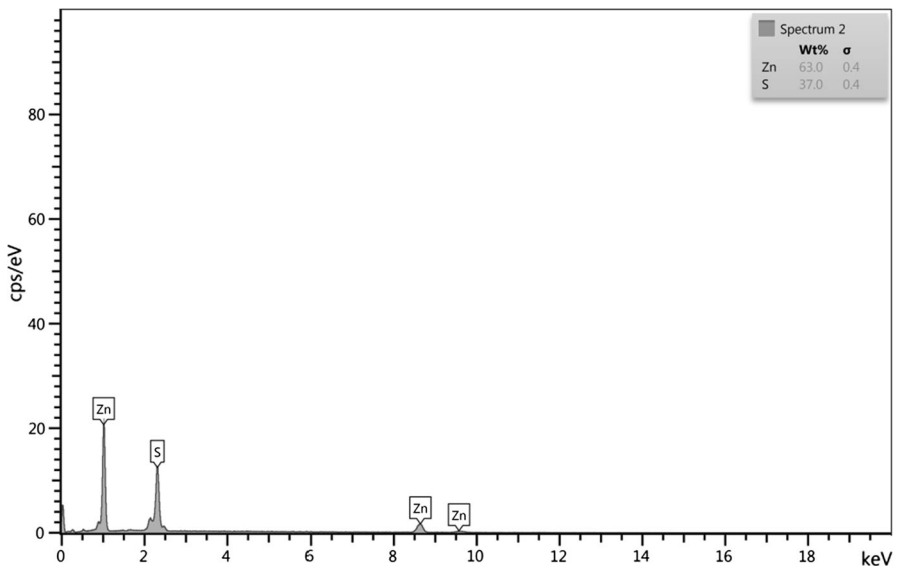


Fig. 5 The EDX spectrum of ZnS NPs catalyst

from the XRD results by Scherrer's equation, $D = k\lambda/\beta\cos\theta$, where k is a constant (generally considered as 0.94), λ is the wavelength of Cu K α (1.54 Å), β is the corrected diffraction line full-width at half-maximum (FWHM), and θ is Bragg's angle. Average size of the prepared ZnS NPs has been found to be 6 nm. X-ray powder diffraction (XRPD)-spectra showed the Bragg reflections for ZnS NPs centered at 2θ : The broad hump 28.8° (1 1 1), 48.2° (2 2 0) and 57.2° (3 1 0).

Electron diffraction X-ray (EDX) analysis

The chemical composition of the product was further examined with energy dispersive X-ray spectrometry (EDX). Purity was shown in the spectrum (Fig. 5), the strong peaks of Zn and S, indicating that the products were pure ZnS NPs. A relatively weak O peak in the spectrum probably originates from unavoidable surface-adsorption of oxygen onto the spheres from exposure to air during the sample processing [41–46].

Scanning electron microscopy (SEM) analysis

Typical SEM images depicted that the nanoparticles were randomly oriented with an average 50 nm and were produced at high density. They uniformly covered the entire substrate. The ZnS NPs are disperses of nanometers size and less 50 nm in diameter. Also, SEM images (Fig. 6) of these NPs show clear lattice balls, which confirm their spherical nature [41–46]. The corresponding XRD pattern demonstrates that these NPs all grow along in three dimensions, and EDX spectra indicate that Zn and S are major elements.

Transmission electron microscopy (TEM) analysis

TEM images of ZnS NPs catalyst are shown in Fig. 7. The TEM images of amorphous ZnS NPs showed the particle sizes to be between 20 and 30 nm, respectively, which is also in good agreement with particle size estimated from XRD spectra by applying the Scherrer equation [41–46]. The techniques, XRD and TEM showed similar trend in continuous increment in particle size (20–30 nm). TEM images ZnS NPs showed the narrow range of particle size distribution, except for ZnS NPs, where smaller particles in the range of 5–6 nm and larger particles of 50–60 nm can be seen. There is good correlation between average particle size (calculated by XRD) and average pore-size distribution (TEM) for synthesized materials, but this is possibly a result of aggregation of nano-sized particles, as explained in earlier sections.

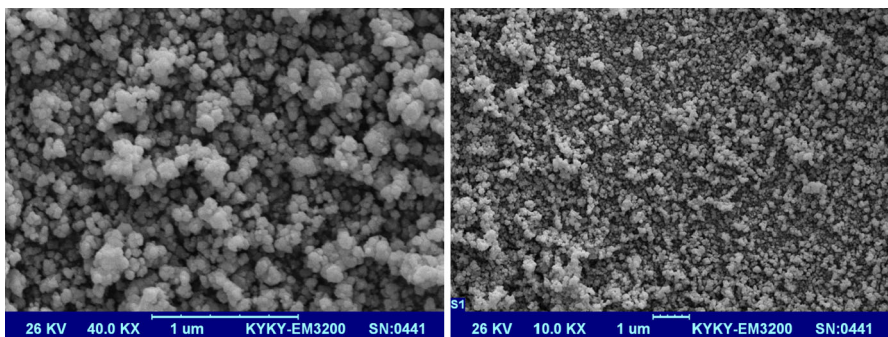


Fig. 6 The SEM of ZnS NPs catalyst

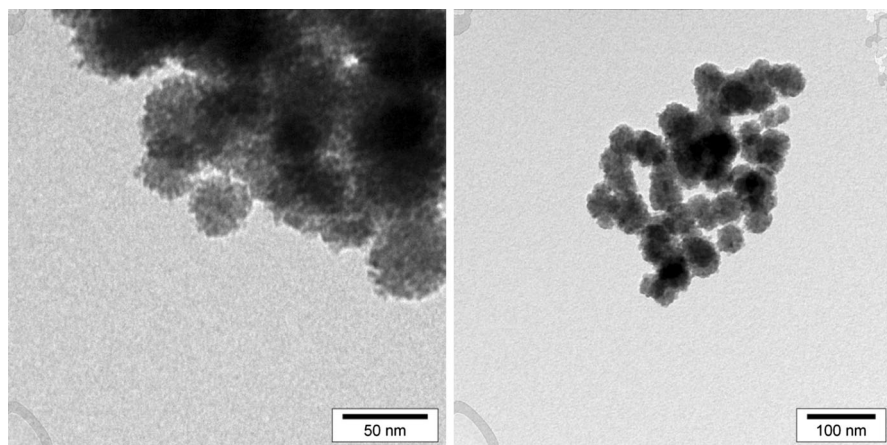


Fig. 7 The TEM image of ZnS NPs catalyst

Table 1 Diverse used catalyst in a model reaction

Entry	Catalyst	Time (min)	Yield ^a (%)
1	MeSO ₃ H	60	40
2	CF ₃ COOH	70	45
3	CuI	55	50
4	Fe ₃ O ₄	50	50
5	MgO	40	31
6	ZnO	35	30
7	ZnS	30	37
8	Zn(CH ₃ COO) ₂ ·2H ₂ O	28	20
9	ZnCl ₂	35	42
10	ZnBr ₂	35	45
11	None	200	30
12	ZnS NPs ^b	19	85

All the reactions were carried out using 10 % mol of catalyst, 1 mmol of *o*-phenylenediamine, 1 mmol of dimedone and 1 mmol of *p*-Cl-benzaldehyde at 70 °C

^a Isolated yields

^b ZnS NPs (10 % mol)

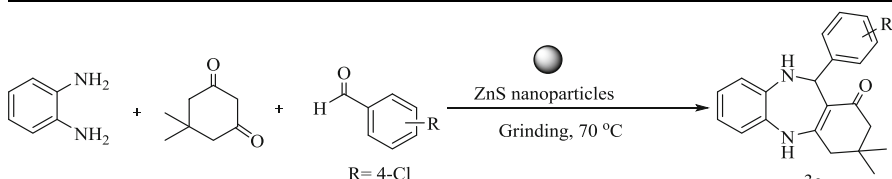
Catalytic studies

The reaction was used in various catalysts such as CF_3COOH , MeSO_3H , Fe_3O_4 , CuI , MgO , ZnO and ZnS ; but none of the above catalysts was found to be more effective than ZnS NPs in this reaction (Table 1). Nevertheless, the reaction at 25°C did not give the desired product and the starting material was recovered, whereas at 55°C , only trace of the desired product was identified by TLC. Also, the reaction was checked in the presence of zinc chloride and zinc bromide salts as catalyst, and the results were added to Table 1, as entries 9, 10. It is clearly shown that the ZnBr_2 and ZnCl_2 are not good catalysts for this reaction, because significant amounts of side products were formed and the main product was very low in yield. It was found that ZnS NPs catalyst was selected for the reaction and the desired product was obtained at 70°C under grinding condition in excellent yield (Table 1, entry 12).

Also, optimization of the temperature and amounts of catalyst in the reaction of dimedone, *o*-phenylenediamine and aromatic aldehydes was selected as the model reaction for one-pot synthesis of the corresponding 1,5-benzodiazepine derivatives. In follow-up research, the model reaction was carried out by using various amounts of ZnS NPs. The optimum amount of ZnS NPs was 10 mol%, as shown in Table 2.

So far, we examined a range variety of aldehydes with various substituents to establish the catalytic importance of ZnS nanoparticles for this reaction. A wide range of 1, 2 and 3-substituted benzaldehydes undergo this one-pot multicomponent synthesis with dimedone and *o*-phenylenediamine toward 4-substituted-1,5-benzodiazepine in high yields (Table 3). In all cases, we observed the almost same performance towards this cyclo condensation to give the desired product (Table 3).

Table 2 Optimization of catalyst amount in the reaction



Entry	Catalyst loading (g)	Time (min)	Yield ^a (%)
1	0.005	17	35
2	0.008	16	55
3	0.01	19	85
4	0.013	19	85
5	0.015	18	84

All the reactions were carried out using 1 mmol of *o*-phenylenediamine, 1 mmol of dimedone and 1 mmol of benzaldehyde at 70°C

^a Isolated yields

Table 3 Synthesis of 4-substituted-1,5-benzodiazepine (3a-o) catalyzed by ZnS nanoparticles under grinding condition

Entry	Aldehyde	Product	Time (min)	Yield ^a (%)	Lit. [30–40] Mp.(°C)	Found M.p. (°C)	TON/TOF (min ⁻¹)
1	C ₆ H ₅		18	84	250–252	246–248	13,520/0.075
2	<i>p</i> -NO ₂ -C ₆ H ₄		17	89	274–275	280–281 ^b	12,020/0.092
3	<i>o</i> -NO ₂ -C ₆ H ₄		17	88	115–117 ^b	230–232 ^b	13,480/0.096
4	<i>m</i> -NO ₂ -C ₆ H ₄		16	88	161–168	195–197	16,550/1.101
5	<i>p</i> -Cl-C ₆ H ₄		19	85	235–237	235–237	14,560/0.975

Table 3 continued

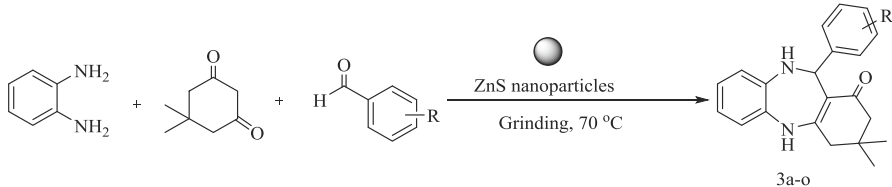
ZnS nanoparticles
Grinding, 70 °C

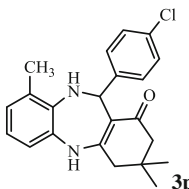
3a-o

Entry	Aldehyde	Product	Time (min)	Yield ^a (%)	Lit. [30–40] Mp.(°C)	Found M.p. (°C)	TON/TOF (min ⁻¹)
6	<i>o</i> -Cl-C ₆ H ₄		22	86	233–235 ^b	239–240 ^b	15,280/ 0.955
7	2,3-Cl-C ₆ H ₃		19	89	–	256–258 ^b	14,820/ 1.058
8	2,4-Cl-C ₆ H ₃		21	90	252	230–232 ^b	12,880/ 0.920
9	4-Cl-3-NO ₂ -C ₆ H ₃		17	87	–	196–197	14,550/ 0.970
10	<i>p</i> -Me-C ₆ H ₄		19	85	157–158 ^b	224–226	16,200/ 1.012

Table 3 continued

Entry	Aldehyde	Product	Time (min)	Yield ^a (%)	Lit. [30–40] Mp.(°C)	Found M.p. (°C)	TON/TOF (min ⁻¹)
11	<i>p</i> -OMe-C ₆ H ₄		18	82	203–205	229–231	15,800/0.877
12	<i>o</i> -OMe-C ₆ H ₄		23	83	213–215 ^b	217–218 ^b	16,700/0.982
13	<i>m</i> -OMe-C ₆ H ₄		25	84	–	225–227	16,510/0.971
14	<i>o</i> -OH-C ₆ H ₄		22	84	164–166	201–202	16,580/0.921
15	<i>m</i> -OH-C ₆ H ₄		23	81	–	287–289 ^b	14,230/0.748

Table 3 continued


Entry	Aldehyde	Product	Time (min)	Yield ^a (%)	Lit. [30–40] Mp.(°C)	Found M.p. (°C)	TON/TOF (min ⁻¹)
16 ^c	<i>p</i> -Cl-C ₆ H ₄		26	80	–	230–234	14,028/ 0.884

All the reactions were carried out using 10 mol% of catalyst, 1 mmol of *o*-phenylenediamine, 1 mmol of dimedone and 1 mmol of *p*-Cl-benzaldehyde at 70 °C

^a Isolated yields

^b Decomposition point

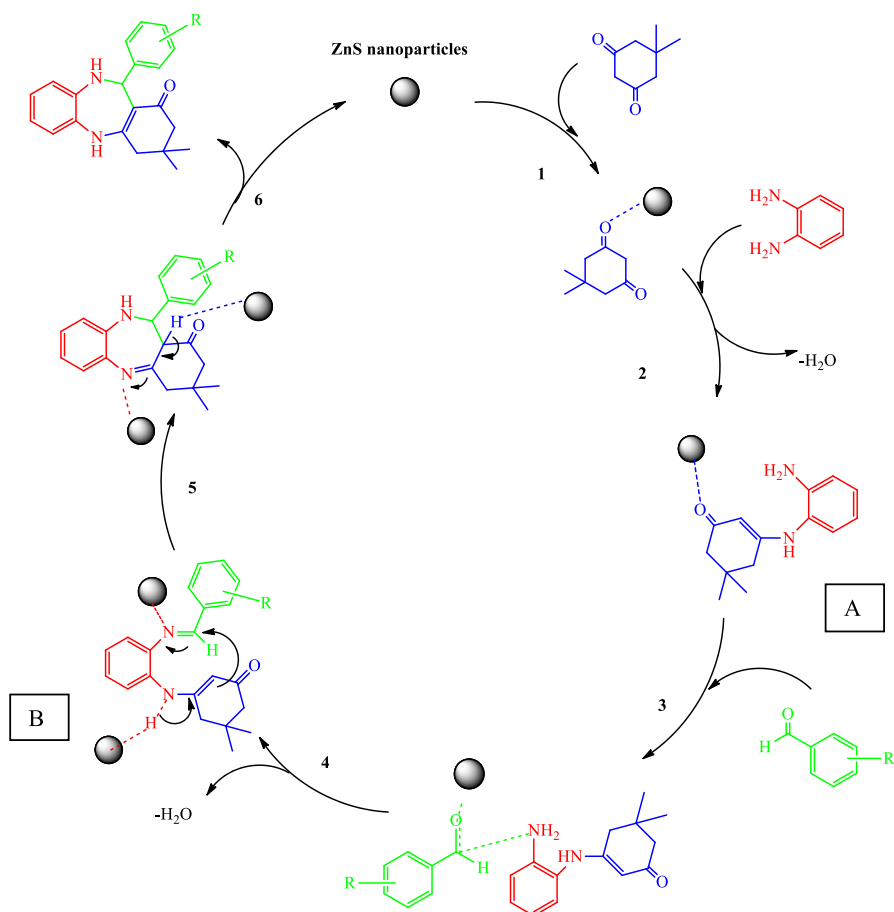
^c The amine substrate for this reaction was 2,3-diaminotoluene

Aliphatic aldehydes gave the corresponding 4-substituted-1,5-benzodiazepine in lower yield (15–20 %) than aromatic aldehydes (81–90 %). Moreover, the 2,3-diaminotoluene was used as diamine substrate in this protocol (Table 3, entry 16), and the results showed high yield of the related product in this reaction. All the synthesized 4-substituted-1,5-benzodiazepines have been characterized on the basis of elemental and spectral studies.

The structure of the obtained products was confirmed by FT-IR, ¹H NMR, ¹³C NMR and EI-MASS spectroscopic data. The FT-IR spectrum of the **3i** as an example exhibited a broad band at 3305 and 3240 cm⁻¹ that is related to amine protons (2 NH groups), bands at 3039 and 2958 cm⁻¹ related to CH, CH₂, and CH₃ groups, and strong bands at 1600 and 1381 cm⁻¹, representing the presence of general carbonyl groups (C=O stretching). Strong bands at 1532 and 1339 cm⁻¹ in FT-IR spectrum confirm the presence of C–N stretching, a band at 1426 cm⁻¹ is related to C=C stretching band, and a strong band at 1276 cm⁻¹ confirms the presence of C–O bond stretching. In addition, the ¹H NMR spectrum of compound **3i** exhibited two singlet bands for two methyl groups at $\delta = 1.02$ ppm and $\delta = 1.07$ ppm, a AB quartet signal at $\delta = 2.13$ ppm with $J = 16.0$ Hz was shown for CH₂ protons. Also, a signal at $\delta = 2.54$ ppm for CH₂–C=O protons and a signal at $\delta = 5.77$ ppm for NH proton are observable. The CH proton was shown at $\delta = 6.08$ ppm, aromatic protons at $\delta = 6.50$ – 7.68 ppm, and NH proton at $\delta = 8.74$ ppm. Also, the ¹³C NMR spectrum of compound **3i** was shown to have distinct 21 carbons, in agreement with proposed structure. Finally, the mass spectra of product **3i** displayed a molecular ion peak at the appropriate m/z value [11, 26].

One heterogeneous catalyst that has obtained attention is ZnS NPs. This excellent particle shows remarkable activity and selectivity for the coupling of aldehydes with dimedone and *o*-phenylenediamine by increasing the surface area and decreasing size. The lower stability of the ZnS-H bond and a special effect between the acid–base properties of ZnS sites found in the reaction are still essential for high yields. Grinding condition was even required and the addition of Lewis acid ZnS NPs was necessary to facilitate the reaction.

The formation of 4-substituted-1,5-benzodiazepine from *o*-phenylenediamine, dimedone and aldehyde in the presence of ZnS NPs as catalyst can be explained by a tentative mechanism that is presented in Scheme 2. One molecule of dimedone (**1**) was firstly condensed with an activated *o*-phenylenediamine (**2**) to provide intermediate **A** and water, which can be regarded as a fast Knoevenagel addition. Then, the active molecule of aromatic aldehyde (**3**) reacted with intermediate **A** via conjugate Michael addition to produce the intermediate **B** and water, which undergoes intramolecular cyclodehydration to give the 4-substituted-1,5-benzodiazepine (**5, 6**).



Scheme 2 Proposed reaction mechanism

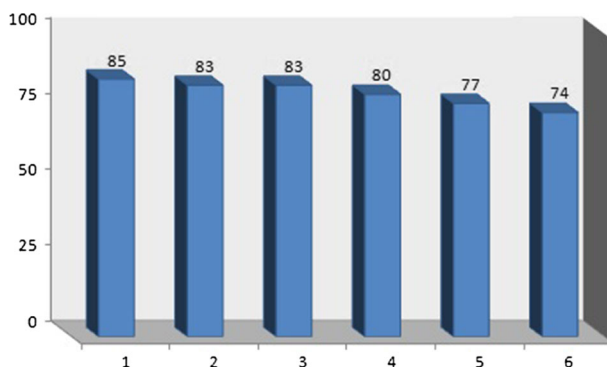


Fig. 8 Reusability of ZnS NPs

Finally, we surveyed catalyst reusability in the MCRs of benzaldehyde with dimedone and *o*-phenylenediamine as a model reaction under the optimized reaction condition. After completion of the reaction, the reaction mixture was dissolved in ethanol and the catalyst was insoluble in ethanol and centrifuged to separate. The ZnS nanoparticles were washed three to four times with ethylacetate and dried at 60 °C for 1 h. The recycled catalyst could be reused five times without any decrease in catalytic activity so that the yields were ranged from 85 to 74 % (Fig. 8).

Conclusion

In the present work, ZnS nanoparticles were prepared and well characterized. The obtained ZnS nanoparticles play a role in the reaction mechanism for three-component coupling of *o*-phenylenediamine, dimedone and aldehydes in order to synthesize some heterocyclic compounds. The pure products were obtained in high yields and short reaction times. The Lewis acidity of the catalyst plays significant role in catalysis, and on the basis of our knowledge, enhancing the rate and yield of the reaction by providing the interfacial bonds between the heterogeneous catalyst and substrates could be performed.

Acknowledgments The authors are grateful to University of Kashan for supporting this work by Grant No.: 159148/49.

References

1. W.T. Yao, S.H. Yu, Q.S. Wu, *Adv. Funct. Mater.* **17**, 623–631 (2007)
2. S. Senthilkumar, R.T. Selvi, *Appl. Phys. A* **94**, 123–129 (2009)
3. K. Kumaravel, G. Vasuki, *Curr. Org. Chem.* **13**, 1820–1841 (2009)
4. L. Banfi, A. Basso, L. Giardini, R. Riva, V. Rocca, G. Guanti, *Eur. J. Org. Chem.* **2011**, 100–109 (2011)
5. M.S. Singh, S. Chowdhury, *RSC Adv.* **2**, 4547–4592 (2012)
6. L.A. Thompson, J.A. Ellman, *Chem. Rev.* **96**, 555–600 (1996)
7. G. Imani Shakibaei, A. Feiz, A. Bazgir, *C. R. Chim.* **14**, 556–562 (2011)

8. P.S. Baran, C.A. Guerrero, N.B. Ambhaikar, B.D. Hafensteiner, *Angew. Chem. Int. Ed.* **44**, 606–609 (2005)
9. G.W. Gribble, *J. Chem. Soc. Perkin Trans.* **1**, 1045–1075 (2000)
10. J.B. Bremner, S. Samosorn, *Azepines and their Fused-ring Derivatives*, Taylor Ed. (Elsevier, Oxford, 2008), pp. 1–43
11. E.C. Cortés, A.L.V. Cornejo, O.G.-M. de Cortés, *J. Heterocycl. Chem.* **44**, 183–187 (2007)
12. L. Makaron, C.A. Moran, O. Namjoshi, S. Rallapalli, J.M. Cook, J.K. Rowlett, *Pharmacol. Biochem. Behav.* **104**, 62–68 (2013)
13. Y.-Q. Luo, F. Xu, X.-Y. Han, Q. Shen, *Chin. J. Chem.* **23**, 1417–1420 (2005)
14. B.P. Bandgar, A.V. Patil, O.S. Chavan, *J. Mol. Catal. A: Chem.* **256**, 99–105 (2006)
15. M. Curini, F. Epifano, M.C. Marcotullio, O. Rosati, *Tetrahedron Lett.* **42**, 3193–3195 (2001)
16. M. Kodomari, T. Noguchi, T. Aoyama, *Synth. Commun.* **34**, 1783–1790 (2004)
17. P.S. Salve, D.S. Mali, *J. Chem. Pharm. Res.* **5**, 158–161 (2013)
18. M.R. Shushizadeh, N. Dalband, *Jundishapur J. Nat. Pharm. Prod.* **7**, 61 (2012)
19. K. Murai, R. Nakatani, Y. Kita, H. Fujioka, *Tetrahedron* **64**, 11034–11040 (2008)
20. X.-Q. Pan, J.-P. Zou, Z.-H. Huang, W. Zhang, *Tetrahedron Lett.* **49**, 5302–5308 (2008)
21. A. Vijayasankar, S. Deepa, B. Venugopal, N. Nagaraju, *Chin. J. Catal.* **31**, 1321–1327 (2010)
22. A. Maleki, *Tetrahedron* **68**, 7827–7833 (2012)
23. G. Maiti, U. Kayal, R. Karmakar, R.N. Bhattacharya, *Tetrahedron Lett.* **53**, 1460–1463 (2012)
24. R. Kaoua, B. Nedjar-Kolli, T. Roisnel, Y. Le Gal, D. Lorcy, *Tetrahedron* **69**, 4636–4640 (2013)
25. O.I. El-Sabbagh, S.M. El-Nabhty, *Bull. Korean Chem. Soc.* **30**, 1445–1449 (2009)
26. E.C. Cortés, M.A. Baños, O.G.-M. De Cortés, *J. Heterocycl. Chem.* **41**, 277–280 (2004)
27. J.N. Sangshetti, R.S. Chouthe, M.R. Jadhav, N.S. Sakle, A. Chabukswar, I. Gonjari, S. Darandale, D.B. Shinde, *Arab. J. Chem.* (2013). doi:[10.1016/j.arabjc.2013.04.004](https://doi.org/10.1016/j.arabjc.2013.04.004)
28. S.-L. Wang, C. Cheng, F.-Y. Wu, B. Jiang, F. Shi, S.-J. Tu, T. Rajale, G. Li, *Tetrahedron* **67**, 4485–4493 (2011)
29. I. Tolpygin, N. Mikhailenko, A. Bumber, E. Shepelenko, U. Revinsky, A. Dubonosov, V. Minkin, *Russ. J. Gen. Chem.* **82**, 1243–1249 (2012)
30. N. Tonkikh, A. Strakovs, K. Rizhanova, M. Petrova, *Chem. Heterocycl. Compd.* **40**, 949–955 (2004)
31. A. Y. Strakov, M. Petrova, N. Tonkikh, A. Gurkovskii, Y. Popelis, G. Kreishman, S. Belyakov, *Chem. Heterocycl. Compd.* **33**, 321–332 (1997)
32. N.J. Parmar, H.A. Barad, B.R. Pansuriya, S.B. Teraiya, V.K. Gupta, R. Kant, *Bioorg. Med. Chem. Lett.* **22**, 3816–3821 (2012)
33. M. Nardi, A. Cozza, A. De Nino, M. Oliverio, A. Procopio, *Synthesis* **2012**, 800–804 (2012)
34. B. Jiang, Q.-Y. Li, H. Zhang, S.-J. Tu, S. Pindi, G. Li, *Org. Lett.* **14**, 700–703 (2012)
35. J. Qian, Y. Liu, J. Cui, Z. Xu, *J. Org. Chem.* **77**, 4484–4490 (2012)
36. P. Guo, X. Zeng, S. Chen, M. Luo, *J. Organomet. Chem.* **751**, 438–442 (2014)
37. M.A. Ghasemzadeh, N. Ghasemi-Seresht, *Res. Chem. Intermed.* (2015). doi:[10.1007/s11164-014-1915-z](https://doi.org/10.1007/s11164-014-1915-z)
38. L.D. Fader, R. Bethell, P. Bonneau, M. Bös, Y. Bousquet, M.G. Cordingley, R. Coulombe, P. Dero, A.-M. Faucher, A. Gagnon, N. Goudreau, C. Grand-Maitre, I. Guse, O. Hucke, S.H. Kawai, J.-E. Lacoste, S. Landry, C.T. Lemke, E. Malenfant, S. Mason, S. Morin, J. O'Meara, B. Simoneau, S. Titolo, C. Yoakim, *Bioorg. Med. Chem. Lett.* **21**, 398–404 (2011)
39. D. McGowan, O. Nyanguile, M.D. Cummings, S. Vendeville, K. Vandyck, W. Van den Broeck, C.W. Boutton, H. De Bondt, L. Quiryne, K. Amssoms, J.-F. Bonfanti, S. Last, K. Rombauts, A. Tahri, L. Hu, F. Delouvroy, K. Vermeiren, G. Vandercruyssen, L. Van der Helm, E. Cleiren, W. Mostmans, P. Lory, G. Pille, K. Van Emelen, G. Fanning, F. Pauwels, T.-I. Lin, K. Simmen, P. Raboisson, *Bioorg. Med. Chem. Lett.* **19**, 2492–2496 (2009)
40. J. Schimer, P. Cigler, J. Veselý, K. Grantz Šašková, M. Lepšík, J. Brynda, P. Řezáčová, M. Kožíšek, I. Císařová, H. Oberwinkler, H. Kraeußlich, J. Konvalinka, *J. Med. Chem.* **55**, 10130–10135 (2012)
41. B. Liu, Q. Liu, C. Tong, X. Lü, C. Lü, *Colloids Surf. Physicochem. Eng. Asp.* **434**, 213–219 (2013)
42. F.A. La Porta, M.M. Ferrer, Y.V. de Santana, C.W. Raubach, V.M. Longo, J.R. Sambrano, E. Longo, J. Andres, M.S. Li, J.A. Varela, *J. Alloys Compd.* **556**, 153–159 (2013)
43. H.-F. Shao, X.-F. Qian, Z.-K. Zhu, *J. Solid State Chem.* **178**, 3522–3528 (2005)
44. M. Navaneethan, J. Archana, K.D. Nisha, S. Ponnusamy, M. Arivanandhan, Y. Hayakawa, C. Muthamizhchelvan, *Mater. Lett.* **66**, 276–279 (2012)
45. D. Xiang, Y. Zhu, Z. He, Z. Liu, J. Luo, *Mater. Res. Bull.* **48**, 188–193 (2013)
46. X.Y. Kong, Z.L. Wang, *Nano Lett.* **3**, 1625–1631 (2003)